Theoretical Possibility of the Variety of Ground-State Spin Arrangements Created by the Spin Hole and Spin Cap in a π-Conjugated System

Ikuya Hagiri, Norihiko Takahashi, and Kyozaburo Takeda*

Department of Materials Science and Engineering, Waseda University, Tokyo 169-8555, Japan

Received: April 17, 2003; In Final Form: December 26, 2003

We have theoretically studied the stable spin state of selected heteroatom-substituted π-conjugated systems. We employed several treatments of Hückel approaches, ab initio calculations, and a Neel state (Heisenberg−Ising) model consideration. All of them elucidate the fact that the different heteroatom arrangements in the π system cause the different spin-stable states of the singlet and the triplet. The possibility of the singlet−triplet instable state is further predicted. These treatments also reveal that the π-electron deficiency due to the replaced group III atom functions as a spin hole and that the excess π electron due to the replaced group V atom functions as a spin cap. We theoretically demonstrate these features via quinodimethane isomers in which two carbon atoms are replaced by heteroatoms, boron and nitrogen.

I. Introduction

Recently, a great deal of interest has been focused on molecular magnetism including nonmagnetized atoms.[1] Many challenging studies have been carried out experimentally as well as theoretically in this field.[2] The utilization of degenerate nonbonding molecular orbitals (NBMOs) is one of the crucial guiding principles in realizing those molecules. The degeneracy of these NBMOs is, however, not caused by molecular symmetry but by a topological peculiarity; therefore, this degeneracy disappears except for the simple Hückel consideration. Nevertheless, these molecules provide a higher-spin (HS) nature. That is, the existence of degenerate NBMOs is not always a "necessary and sufficient" condition for the HS ground-state formation. Rather, an essential factor in the one-electron scheme is whether an induced exchange interaction overcomes the corresponding excitation energy. Thus, one can expect the HS ground state in such a system to have quasi-degenerate π MOs.

Because the heteroatom substitution changes atomic on-site energies, some quasi-degeneracies are accidentally provided in the resulting MOs. From this viewpoint, many π-conjugated materials have been theoretically proposed, and substantial heteroatom doping has been experimentally challenged. We also have studied theoretically whether or how heteroatom substitution changes the stable spin state in the π-conjugated system.[3] We have assumed a model π system of heteroatom-substituted naphthalene and have found the theoretical possibility of the HS stable state as well as quasi-degeneracies of π MOs when the heteroatom boron (B) is incorporated. Furthermore, we have found that the π-electron deficiency of replaced heteroatom B functions as a spin hole for the parent π-electron system.

For a systematic understanding of the heteroatom substitution in the π-conjugated system, one should further study such heteroatom replacement using group V elements because the latter elements produce an excess π electron in the sp^2 network system. This excess π electron forms a local pair in the π system; therefore, it tends to localize at its own atomic site while maintaining an opposite spin arrangement. Consequently, these local pairs of π electrons are expected to be spinless for the parent π-electron network (spin cap). Thus, the replacement by the heteroatom functions as if the group III element digs a hole or the group V element puts a cap along the π-electron path.

For the first step in elucidating the electronic role of these π spin holes and spin caps, we here theoretically study the stable-spin ground state via a discussion of the selected heteroatom-substituted model π system. We assume such a π-conjugated system based on quinodimethane (QDM) including a π spin hole/spin cap pair. QDM ($C_6H_4(CH_2)_2$) itself causes three types of structural isomers of ortho(o), para(p), and meta(m) types. Up to the present time, a great deal of theoretical work on these QDMs has been extensively carried out: Following the pioneering works by Borden and Davidson[4] and Ovchinnikov,[5] Döhnert and Koutecký[6] have carried out quantum chemistry calculations by using the Pariser−Parr−Pople approach. Flynn and Michl[7] have studied the effect of electron correlation. Kato et al.[8] and Fort et al.[9] have carried out more elaborate ab initio calculations. Karafiloglou[10] has also intensively studied the singlet−triplet coupling in xylylnes. On the contrary, very little work has been carried out on those selected heteroatom-substituted QDMs. Here, two of the skeletal carbon atoms are replaced by a heteroatom, producing a spin hole or a spin cap. Therefore, 28 different isomers result for *o*-QDMs, and 29 and 17 isomers are produced for *m*- and *p*-QDMs, respectively. Thus, this system has the following advantages: the resulting structural variety involves typical edge forms of zigzag, armchair, and so forth, whose topological peculiarity causes the characteristic π-electronic features. The incorporation of a spin hole/spin cap pair also conserves the total π-electron numbers as well as charge neutrality.

In the following discussion, we first estimate the ground-state spin arrangement based on the Hückel consideration by the Longuet-Higgins (LH)[11] rule and also the simple valence bond (SVB) approach.[5] We then compare those predictions with those by ab initio Hartree−Fock calculations. We also obtain the Neel state (Heisenberg model under the Ising approximation) energies by taking into account the π-electron spin delocalization and discuss the variety of ground-state spin arrangements quantitatively. Although the treatments used here are based on conventional considerations and their straightforward employ-

* Corresponding author. E-mail: takeda@waseda.jp.

10.1021/jp0307102 CCC: $27.50
Published on Web 03/03/2004

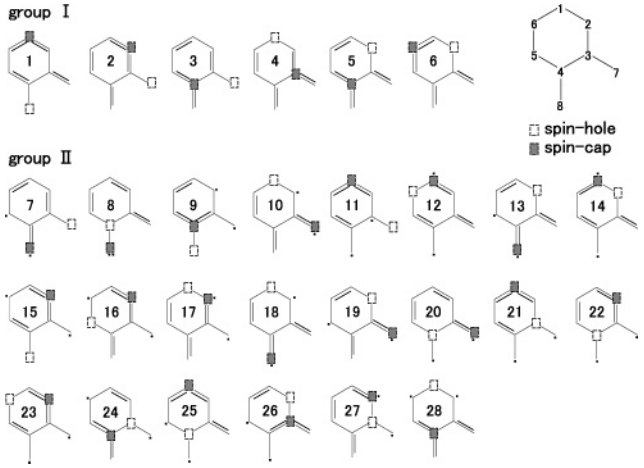

Figure 1. Illustration of possible Kekulé and non-Kekulé forms of the *o*-QDM isomers, which include the π spin hole and spin cap.

ment, it is also our purpose to represent the electronic role of these π spin holes and spin caps in the one-electron scheme, without losing the physical advantages.

II. Hückel Prediction

A. Longuet-Higgins Approach. The Longuet-Higgins (LH) rule[11] is well known to predict a ground spin state of a hydrocarbon π-conjugated system qualitatively on the basis of Hund's rule. According to this rule, the total spin value S of the system is expressed as

$$S = \frac{N - 2T}{2} \tag{1}$$

Here, N and T represent the number of π electrons and the maximum number of double bonds among all possible resonance structures, respectively. Longuet-Higgins has shown that the number of nonbonding molecular orbitals (NBMOs)[12] in the system is $N - 2T$ and has given the value of the total spin by eq 1.

We have applied this LH rule to the present model system of *o*-, *p*- and *m*-QDM isomers including a π spin hole and a π spin cap by extending the meaning of the Kekulé structure.[13] Because all isomers include 8 π electrons, N should be 8. We then draw possible Kekulé structures in order to count the number of double bonds T. We show the case of *o*-QDM isomers in Figure 1a. A full Kekulé structure can be drawn for the isomers of group I. The value of T is, therefore, 4, and the LH rule predicts the ordinary singlet ground state for those group I isomers (Table 1). On the contrary, isomers belonging to group II cannot provide a complete Kekulé structure but rather cause a "biradical" structure. Therefore, the replacement by such heteroatoms of a group III element (π spin hole) and a group V element (π spin cap) and also their arrangement reduce the number of possible double bonds T by 1 ($T = 3$). Thus, the LH rule predicts the existence of a triplet state for these group II isomers. This feature contrasts with the ordinary, homogeneous *o*-QDM because it gives a singlet state uniquely. It is also characteristic that the number of group II isomers is larger than that of the group I isomers.

Similarly, we show the resulting Kekulé and non-Kekulé forms and also the predicted LH spin states for the other heteroatom-substituted isomers having para and meta forms in Figures 2 and 3 and Tables 2 and 3, respectively. A possible triplet state is also expected in the heteroatom-substituted *p*-QDM system. Furthermore, in the *m*-QDM system, this rule

TABLE 1: Predicted LH Spin States for the *o*-QDM Isomers of Figure 1[a]

molecule	LH	SVB	UHF	Neel
1	S	T	T	T
2	S	T	T	T
3	S	S/T	S/T	S/T
4	S	S/T	S/T	S/T
5	S	S/T	S/T	S/T
6	S	S/T	S/T	S/T
17	S	S/T	S/T	S/T
7	T	S	S	S
8	T	S	S	S
9	T	S	S	S
10	T	S	S	S
11	T	S	S	S
12	T	S	S	S
13	T	S	S	S
14	T	S	S	S
15	T	S	S	S
16	T	S	S	S
18	T	T	T	T
19	T	T	T	T
20	T	S/T	S/T	S/T
21	T	S/T	S/T	S/T
22	T	S/T	S/T	S/T
23	T	S/T	S/T	S/T
24	T	S/T	S/T	S/T
25	T	S/T	S/T	S/T
26	T	S/T	S/T	S/T
27	T	S/T	S/T	S/T
28	T	S/T	S/T	S/T

predicts a much higher spin arrangement of a quintet state. Considering that homogeneous *o*- and *p*-QDMs give a singlet state uniquely and the remaining *m*-QDM decisively gives a triplet state, the replacement by the heteroatoms causing a spin hole or spin cap is expected to open the possibility of different spins for the HS and LS stable states in accordance with their heteroatom arrangements.

B. Simple Valence Bond Approach. There is one more simple approach to the prediction of the spin state of a hydrocarbon π-conjugated system, which is known as the simple valence bond (SVB) scheme.[5] The resulting total spin value S for the system is given as follows:

$$S = \frac{|n^* - n|}{2} \tag{2}$$

n^* and n are the numbers of so-called starred and unstarred carbon atoms in the system, respectively. In this SVB scheme, an exchange integral between two adjacent π electrons should be negative so as to arrange their π-electron spins antiparallel.

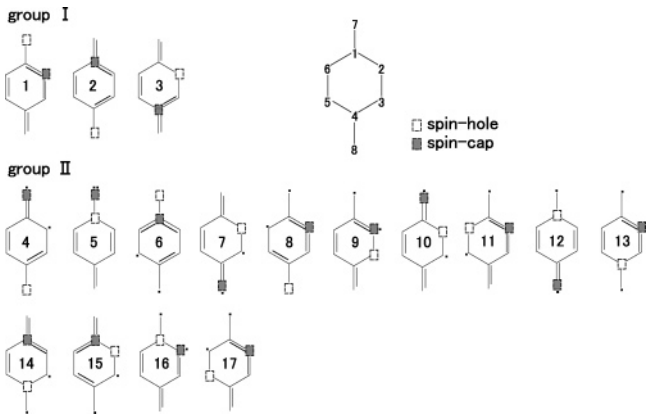

Figure 2. Illustration of possible Kekulé and non-Kekulé forms of the *p*-QDM isomers, which include the π spin hole and spin cap.

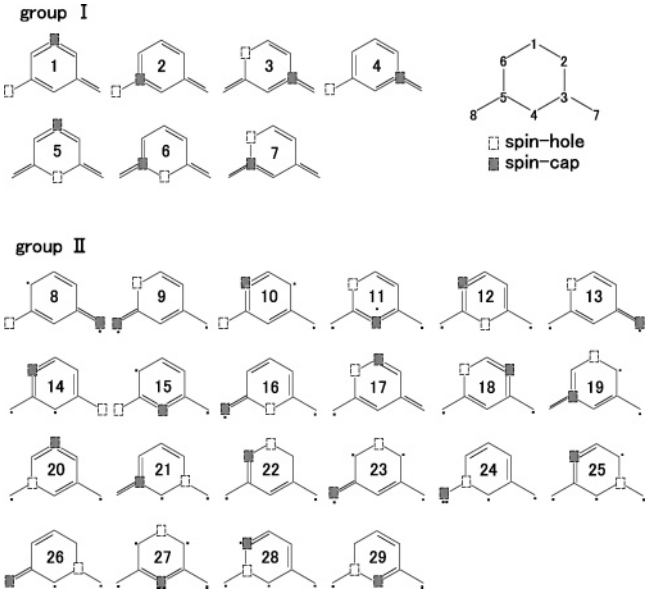

Figure 3. Illustration of possible Kekulé and non-Kekulé forms of the *m*-QDM isomers, which include the π spin hole and spin cap.

TABLE 2: Predicted LH Spin States for the *p*-QDM Isomers of Figure 2[a]

molecule	LH	SVB	UHF	Neel
1	S	T	T	T
2	S	S/T	S/T	S/T
3	S	S/T	S/T	S/T
4	T	S	S	S
5	T	S	S	S
6	T	S	S	S
7	T	S	S	S
8	T	S	S	S
9	T	S	S	S
10	T	T	T	T
11	T	T	T	T
12	T	S/T	S/T	S/T
13	T	S/T	S/T	S/T
14	T	S/T	S/T	S/T
15	T	S/T	S/T	S/T
16	T	S/T	S/T	S/T
17	T	S/T	S/T	S/T

[a] We also show those spin states predicted by the SVB approach, ab initio UHF/6-31G** calculations, and the Neel state consideration.

Therefore, we can directly assign an up spin ($\uparrow$) to the starred carbon and a down spin ($\downarrow$) to the unstarred carbon (or vice versa). This SVB approach is also well known to predict the difference in the ground-state spin among the ordinary homogeneous QDM isomers of the ortho-type (singlet), para-type (singlet), and meta-type (triplet) forms.

By using the valence bond (VB) approach,[14] Klein and his group have extensively studied the electronic structures and magnetic properties of the π-conjugated systems. They have also extended the VB approach and have intensively studied the unpaired π-electron system.[15] We extend this SVB method to the heteroatom-substituted QDM isomers as follows:

- All C atoms are first assigned to starred or unstarred atoms alternately. Successively, up spins are put on the starred atoms, and down spins are put on the unstarred atoms.
- The spin arrangement on the spin hole or spin cap atom is, however, excluded because the spin-hole atom (group III) has no π electron but the spin-cap atom has a local pair of π electrons providing no π spin.

This approach has an advantage over the LH rule because it determines the spin arrangement, in addition to its total spin

TABLE 3: Predicted LH Spin States for the *m*-QDM Isomers of Figure 3[a]

molecule	LH	SVB	UHF	Neel
1	S	T	T	T
2	S	T	T	T
3	S	S/T	S/T	S/T
4	S	S/T	S/T	S/T
5	S	S/T	S/T	S/T
6	S	S/T	S/T	S/T
7	S	S/T	S/T	S/T
8	T	S	S	S
9	T	S	S	S
10	T	S	S	S
11	T	S	S	S
12	T	S	S	S
13	T	S	S	S
14	T	S	S	S
15	T	S	S	S
16	T	T	T	T
17	T	S/T	S/T	S/T
18	T	S/T	S/T	S/T
19	T	S/T/Q	S/T	S/T
20	T	S/T/Q	S/T	S/T
21	T	S/T/Q	S/T	S/T
22	Q	T	T	T
23	Q	T	T	T
24	Q	T	T	T
25	Q	S/T	S/T	S/T
26	Q	S/T	S/T	S/T
27	Q	S/T	S/T	S/T
28	Q	S/T	S/T	S/T
29	Q	S/T	S/T	S/T

[a] We also show those spin states predicted by the SVB approach, ab initio UHF/6-31G** calculations, and the Neel state consideration.

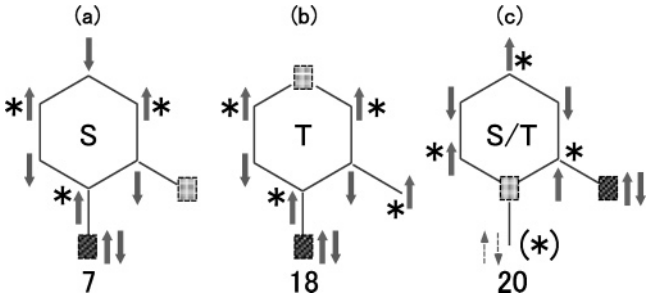

Figure 4. Possible spin arrangement for heteroatom-substituted *o*-QDM isomers (a) **7**, (b) **18**, and (c) **20** estimated by the SVB approach. At the bottommost site in isomer **20** (c), the spin direction is not uniquely determined. We illustrate this feature by the broken arrows.

value. Furthermore, an interesting point is that this SVB approach predicts an instability between the singlet and triplet states or among those much higher (quintet) states. These features are never found by the LH rule. We examine those by examples of the above *o*-QDM isomers **7**, **18**, and **20**, which include the spin hole and spin cap. The SVB approach predicts a singlet state for isomer **7**, and the possible spin arrangement is shown in Figure 4a. This result is in contrast to that obtained by the LH rule, which predicts a triplet state. On the contrary, for isomer **18** (Figure 4b), the SVB approach predicts a triplet state, as the LH rule predicts. Furthermore, one should notice that an indefinite *S* value of 0 or 1 is given for isomer **20**. This indefiniteness of the *S* value originates from the unsettled marking of the star or the unstar at the exocyclic C atom (Figure 4c). Thus, isomer **20** is supposed to cause instability between the singlet and triplet states. This spin-unstable state is a novel phase that is created by the π spin hole and π spin cap accompanied by the replaced heteroatom of the group III and V atoms, respectively, but it never appears in the ordinary

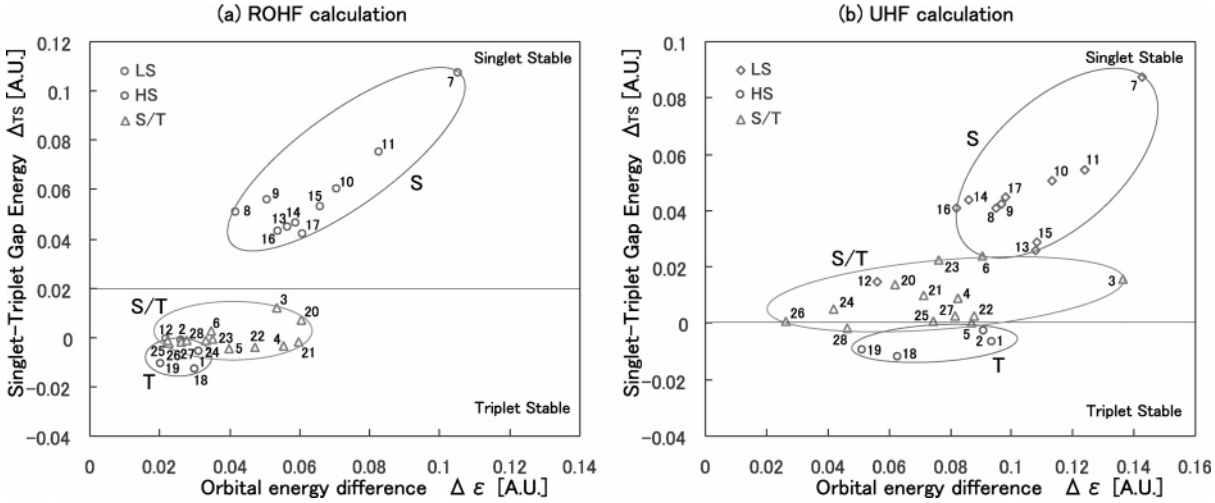

Figure 5. Singlet−triplet energy gaps of B (spin hole)- and N (spin cap)-replaced *o*-QDM obtained by (a) ROHF/6-31G** and (b) UHF/6-31G** calculations, respectively.

homogeneous *o*-QDM. We summarize the possible spin states for the heteroatom-substituted *o*-, *p*-, and *m*-QDM isomers in Tables 1−3, respectively.

III. Ab Initio Calculations

Thus, the above two conventional (Hückel-like) approaches predict the possible multiphases of the spin-stable state for the heteroatom-substituted QDM isomers. However, details in the predictions are different between the two approaches. Therefore, we quantitatively elucidate several ambiguities by performing ab initio calculations of the total energies for all of the isomers while changing their spin configurations. In ab initio calculations, we should set the specific atoms to the π spin hole and spin cap. Here, we assume heteroatom B to be the π spin hole of the group III element and heteroatom N to be the π spin cap of the group V element.

In Figure 5a, we show those ab initio total energies of the BN-replaced *o*-QDM isomers (**1**−**28**) calculated by the restricted open-shell Hartree−Fock (ROHF) approach. In the calculations, the individual isomers are geometrically optimized while maintaining the planarity in order to conserve their distinct π electrons.[16] We also represent the resulting energies in terms of a difference between singlet and triplet states (singlet−triplet gap energy, $\Delta_{TS} = E_T - E_S$). Thus, a positive value of Δ_{TS} means that the singlet state is more stable than the triplet, and a negative value means the triplet state is more stable. In the figures, we also represent the horizontal axis by the difference $\Delta\epsilon$ in the orbital energies between the HOMO and HOMO-1 of the triplet state for the individual isomers.[17] Because this difference $\Delta\epsilon$ corresponds roughly to the one-electron excitation energy, a singlet state is predicted with an increase in $\Delta\epsilon$, and a triplet state is expected with a decrease in $\Delta\epsilon$. One can then also expect a positive slope in the calculated Δ_{TS} versus $\Delta\epsilon$ plot.

Pure *o*-QDM is well known to show a singlet ground state uniquely. However, one can find that several BN-substituted *o*-QDM isomers have a negative Δ_{TS} value. A triplet state is well predicted for **1**, **2**, **18**, and **19** (symbol ○). Thus, the present ROHF calculation surely predicts the existence of other possible spin phases besides the conventional singlet state. Moreover, we notice that the ROHF results are in agreement with the classification by the SVB approach rather than that by the LH rule: For example, the SVB approach predicts isomers **7**−**17** to be classified into the singlet-state group, and the remainder **3**−**6** and **20**−**28** cause instability between the singlet and triplet states. The present ab initio ROHF calculations surely classify isomers **7**−**17** (symbol ◇) into the singlet-state group because of their positive Δ_{TS} values. Furthermore, the resulting small Δ_{TS} values quantitatively lead to the singlet−triplet (S/T) instability for isomers **3**−**6** and **20**−**28** (symbol △), as suggested by the SVB approach. An inconsistency is found for isomer **12** only. The SVB approach predicts that the former causes a singlet state, but the ROHF/6-31G** calculation predicts an S/T instability.

We also calculated these ab initio singlet−triplet gap energies by the unrestricted Hartree−Fock (UHF) approach (Figure 5b) in order to incorporate the effects of spin polarization as well as spin delocalization, more precisely. In accordance with the Δ_{TS} value being positive, negative, and almost zero, the UHF calculation also classifies the isomers into three groups more consistently as well as distinctly, such as singlet (S), triplet (T), and singlet−triplet (S/T) unstable species: The Δ_{TS} value for isomer **12** is reasonably increased now, although it still remains in the region of the S/T unstable phase. In the UHF calculations, isomers predicted to cause S/T instability also produce a nearly zero value of Δ_{TS}, except for a few that are distributed with small values of Δ_{TS}. Furthermore, one should notice that both of the present ab initio results show good positive-slope character in the Δ_{TS} versus $\Delta\epsilon$ plot.

Quite similar results are also found both in BN-replaced *p*- and *m*-QDM isomers as shown in Figures 6 and 7, respectively. Thus, the ab initio HF results reveal that the existence of a π spin hole and spin cap, and their geometrical arrangement surely increases the variety in the spin ground states. It is also confirmed that the present SVB approach provides a consistent prediction for the ground-state spin.

IV. Neel State Energy Consideration

A. Neel State (Ising Spin) Approximation. Here, we discuss the possible spin states for these isomers from a more rational but quantitative point of view, which is different from that of ab initio calculations. To clarify this subject, we calculate the Neel state (Heisenberg model under the Ising spin approximation)[18] energy for these heteroatom-substituted π isomers.[19]

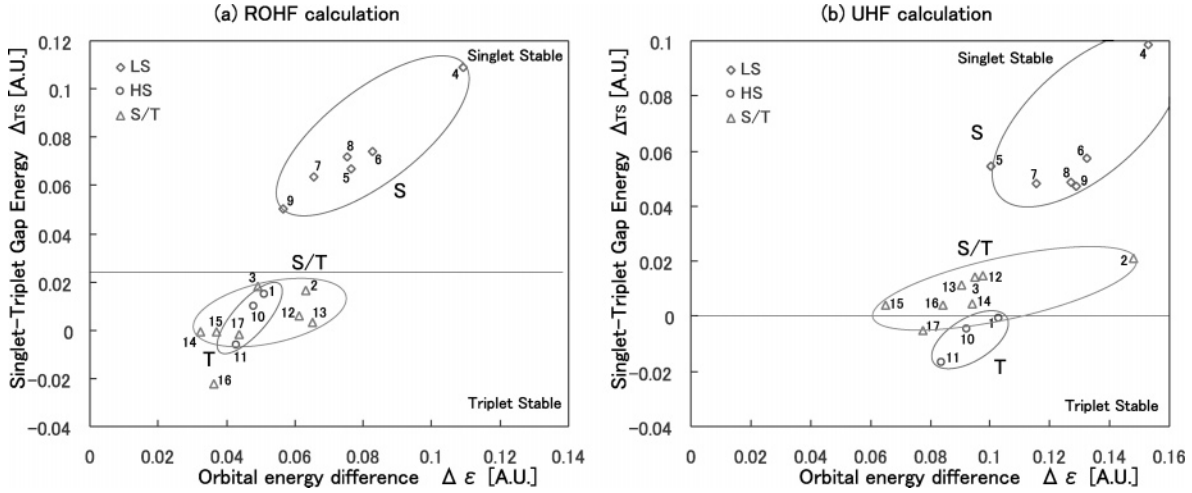

Figure 6. Singlet−triplet energy gaps of B (spin hole)- and N (spin cap)-replaced *p*-QDM. All values are obtained by (a) ROHF/6-31G** and (b) UHF/6-31G** calculations, respectively.

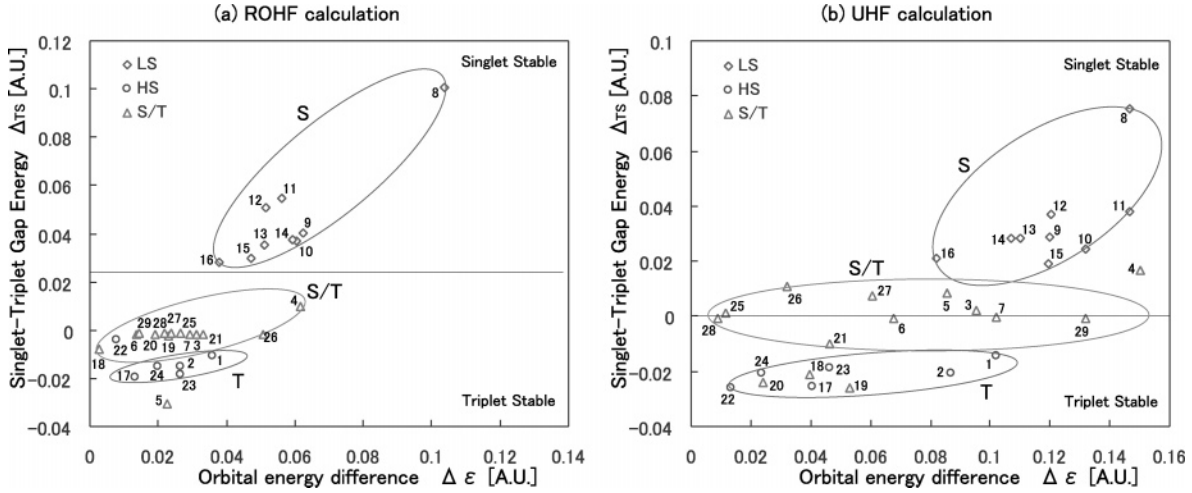

Figure 7. Singlet−triplet energy gaps of B (spin hole)- and N (spin cap)-replaced *m*-QDM obtained by (a) ROHF/6-31G** and (b) UHF/6-31G** calculations, respectively.

We here use the conventional Neel state (Heisenberg−Ising) model Hamiltonian that is given as follows:[20]

$$H = -\sum_{i,j} 2J_{ij}\mu_i \cdot \mu_j \tag{3}$$

μ_i is the π-electron spin on the ith atom site. Under the Ising spin approximation, the sum of i and j should be taken into account between the nearest-neighbor sites, including the zero value for the heteroatom because of its π spin-hole or spin-cap nature. Furthermore, we assume these effective exchange integrals J_{ij} to be equivalent and negative ($J_{ij} = J < 0$).[21]

Thus, eq 3 is rewritten into the following normalized form h:

$$h = \frac{H}{-2J} = \sum_{i,j} \mu_i \cdot \mu_j \tag{4}$$

The stable ground state of a lower-spin (LS) or a higher-spin (HS) state should then be determined only by obtaining such a spin arrangement (set of μ_i) giving a minimum energy of $h^{\mathrm{LS}}_{\mathrm{min}}$ or $h^{\mathrm{HS}}_{\mathrm{min}}$, respectively. However, this minimization should be carried out along with the maintenance of the total spin value of $|n(\uparrow) - n(\downarrow)|$ (e.g., $|n(\uparrow) - n(\downarrow)| = 0$ for a singlet spin (LS) state or $|n(\uparrow) - n(\downarrow)| = 2$ for a triplet spin (HS) state). In Figure 8, we show those resulting spin arrangements giving $h^{\mathrm{T}}_{\mathrm{min}}$ and $h^{\mathrm{S}}_{\mathrm{min}}$ for heteroatom-substituted *o*-QDM isomers **7** (a), **18** (b), and **20** (c), respectively.

For isomer **7**, the condition of the singlet state $|n(\uparrow) - n(\downarrow)| = 0$ reduces all of the possible 64 spin arrangements to 20, and the spin arrangement causing the minimum $h^{\mathrm{S}}_{\mathrm{min}}$ is given as

$$\begin{cases} \mu_1 = \mu_3 = \mu_5 = -1 \\ \mu_2 = \mu_4 = \mu_6 = +1 \\ \mu_7 = \mu_8 = 0 \end{cases} \tag{5}$$

The corresponding Neel state energy $h^{\mathrm{S}}_{\mathrm{min}}$ is then obtained as

$$h^{\mathrm{S}}_{\mathrm{min}} = \mu_1 \cdot \mu_2 + \cdots = -6 \tag{6}$$

Although this spin state is doubly-degenerate, the other 18 remaining spin arrangements except for them give a (singlet) Neel state energy of h^{S} greater than $h^{\mathrm{S}}_{\mathrm{min}} = -6$. One should also notice that this spin arrangement is completely coincident with that predicted by the SVB approach.

Similarly, the restriction of $|n(\uparrow) - n(\downarrow)| = 2$ causes 15 different triplet spin arrangements for isomer **7**. Among them, one can obtain the stable triplet state and its Neel state energy

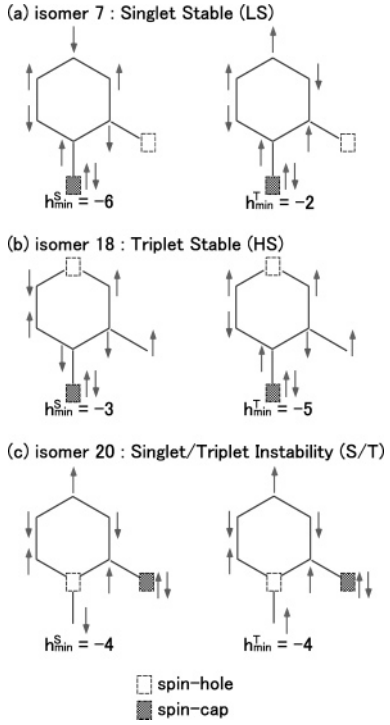

Figure 8. Resulting π-electron spin arrangements of *o*-QDM isomers (a) **7**, (b) **18**, and (c) **20**, which include a π spin hole and spin cap. All of the arrangements are computationally determined under the Neel state (Ising spin) approximation to give a minimum Neel state (Heisenberg−Ising) energy of the singlet and triplet states, respectively. We also show those calculated Neel state energies for the singlet and triplet states.

h^T_{min} as follows:

$$\begin{cases} \mu_1 = \mu_3 = \mu_4 = \mu_6 = +1 \\ \mu_2 = \mu_5 = -1 \\ \mu_7 = \mu_8 = 0 \end{cases} \tag{7}$$

and

$$h^T_{min} = -2 \tag{8}$$

This state is also 9-fold degenerate, but the other six remaining spin arrangements give a (triplet) Neel state energy h^T greater than $h^T_{min} = -2$. Thus, the simple Ising approach reveals that isomer **7** gives $h^S_{min} = -6$ as less than $h^T_{min} = -2$. That is, it predicts that the *o*-QDM in which the π spin hole and spin cap are arranged as the pattern of isomer **7** gives the singlet ground state, being energetically more stable than the triplet by 4 in J units ($h^S_{min} < h^T_{min}$).

Now, we can consider the π spin arrangement of the other *o*-QDM isomers (Figure 8). For heteroatom-substituted *o*-QDM isomer **18** (Figure 8b), for example, the calculated minimum Neel state energies for the singlet and triplet states are $h^S_{min} = -3$ and $h^T_{min} = -5$, respectively. Consequently, the triplet state is predicted to be the ground state for this *o*-QDM isomer **18**. The spin arrangement of this triplet state is also coincident with that predicted by the SVB approach.

What about heteroatoms-replaced *o*-QDM isomer **20**? The present simple Ising approach also gives an equal minimum energy of $h^S_{min} = h^T_{min} = -4$. This *o*-QDM isomer is therefore predicted to cause the singlet−triplet (S/T) instability in its ground state, as the SVB approach estimates and the ab initio calculations elucidate. Thus, we can also classify the possible

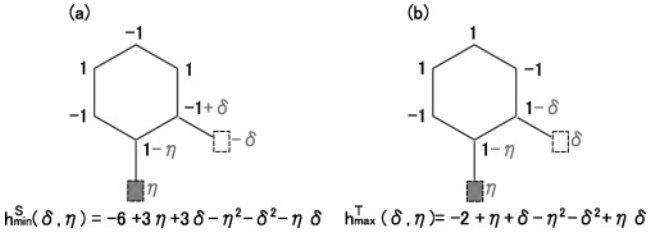

Figure 9. Illustration of the in-flowing (δ) and out-flowing (η) of π-electron spins for the heteroatoms-replaced *o*-QDM isomer of **7**. We give the minimum Neel state energies of the (a) singlet and (b) triplet states. We also show the possible changes in $h^T_{min}(\delta,\eta)$ and $h^S_{min}(\delta,\eta)$ with varying δ and η.

spin ground states of the present heteroatom-substituted QDM isomers into three groups of singlet-spin (LS), triplet-spin (HS), and singlet−triplet (S/T) unstable phase by this Neel state-energy calculation. In Tables 1−3, we can compare those possible spin phases estimated by the Ising spin approximation with those obtained by ab initio calculations as well as the SVB approach. Good agreement is found among them.

B. π-Spin Delocalization by the tJ-Model Consideration. In the above simple Ising spin treatment, π spins are completely localized on the individual parent (carbon) atom sites. However, the replacement of heteroatoms causes charge transfer by which an in-and-out flowing of the π spins occurs and by which the possible spin state might be changed. We therefore take into account this π-spin delocalization and recalculate the Neel state energy. We define a net in-flowing of the π spin into the spin hole or spin cap site by δ ($0 \le \delta \le 1$) or by η ($0 \le \eta \le 1$), respectively. For simplification, these in- and out-flowings of the π spin ($\pm\delta$ and $\pm\eta$) are, however, limited to those mutually bonded atoms between parent (carbon) atoms and/or replaced heteroatom(s), and the other remaining parent atoms have no π-spin transfer ($\delta = \eta = 0$). Thus, following the computational obtainment of all of the possible spin arrangements, we can calculate the minimum Neel state energy for the singlet state (h^S_{min}) or for the triplet state (h^T_{min}) in order to determine the stable spin state.

As mentioned previously, isomer **7** produces 20 different spin-arrangement patterns under the singlet spin state when the following spin arrangement is provided (Figure 9a),

$$\begin{cases} \mu_1 = \mu_5 = -1 \\ \mu_2 = \mu_6 = +1 \\ \mu_3 = -1 + \delta \\ \mu_4 = +1 - \eta \\ \mu_7 = -\delta \\ \mu_8 = \eta \end{cases} \tag{9}$$

the minimum Neel state energy $h^S_{min}(\delta, \eta)$ is obtained as

$$h^S_{min}(\delta,\eta) = -6 + 3\delta + 3\eta - \delta^2 - \eta^2 - \delta\eta \tag{10}$$

Similarly, while maintaining $|n(\uparrow) - n(\downarrow)| = 2$, we should search for the triplet stable spin arrangement of this isomer **7** from 15 different patterns. The resulting minimum Neel state energy for the triplet state $h^T_{min}(\delta,\eta)$ is obtained as

$$h^T_{min}(\delta, \eta) = -2 + \eta + \delta - \eta^2 - \delta^2 + \eta\delta \tag{11}$$

For the other isomers (e.g., **18** and **20**), we also computationally determined the stable spin arrangements of both the singlet and triplet states and analytically obtained their minimum

values of $h^{T}_{min}(\delta, \eta)$ and $h^{S}_{min}(\delta, \eta)$ as follows:

$$h^{S}_{min}(\delta, \eta) = -3 + \eta + 2\delta - \eta^2 \quad (12)$$

$$h^{T}_{min}(\delta, \eta) = -5 + 3\eta + 6\delta - \eta^2 - 4\delta^2 \quad (13)$$

for isomer **18**, and

$$h^{S}_{min}(\delta, \eta) = -4 + 2\eta + 3\delta - \eta^2 - \delta^2 - 2\eta\delta \quad (14)$$

$$h^{T}_{min}(\delta, \eta) = -4 + 2\eta + 11\delta - \eta^2 - 9\delta^2 - 4\eta\delta \quad (15)$$

for isomer **20**.

These analytical expressions of the Neel state energies have the following advantages: Qualitatively, the limitation to the localized π spin ($\delta = \eta = 0$) leads to the present Neel state energies that are equivalent to those estimated by the simple Ising spin approximation. Quantitatively, the contribution due to the π-spin delocalization is understood by an extra δ and η functional of δ^2, η^2 and $\delta\eta$ or less. Moreover, the noticeable point is that these extra terms are quadratic in π-spin delocalization parameters δ and η. Although this quadraticity is caused by the mutual-spin interactions approximated by those between neighboring spins, we can rationally discuss the ground-state spin arrangement for the system having the spin hole(s) and spin cap(s). The reason is that the relative characteristics of any two second-order surfaces are mathematically elucidated. In the present case ($0 \le \delta \le 1$ and $0 \le \eta \le 1$), the resulting two surfaces $h^{S}_{min}(\delta, \eta)$ and $h^{T}_{min}(\delta, \eta)$ should have one crossing line (real roots) except for the case when they have equal roots or imaginary roots due to this quadraticity. Furthermore, on the basis of the present analytical expressions, one can systematically discuss how the π-spin delocalization changes the Neel state energies $h^{S}_{min}(\delta, \eta)$ and $h^{T}_{min}(\delta, \eta)$ by varying δ and η (Figure 10). This change in the π-spin delocalization corresponds to the change in the kinds of replaced atoms.

An arrangement of the π spin hole (group III atom) and π spin cap (group V atom) such as isomer **7** gives no crossings between the two Neel state energy surfaces of the singlet (S) and triplet (T) states, and the relation of $h^{T}_{min}(\delta, \eta) > h^{S}_{min}(\delta, \eta)$ is maintained within any defined π-spin in- and out-flowings ($0 \le \delta \le 1$ and $0 \le \eta \le 1$) as shown in Figure 10a. This feature means that the arrangement of the π spin hole and spin cap equal to isomer **7** should cause a singlet stable ground state rather than a triplet state, even when those sites are replaced by any other heteroatoms ($0 \le \delta \le 1$ and $0 \le \eta \le 1$). The other heteroatom-substituted *o*-QDM isomers classified into the group of the singlet stable phase (group S) also provide a similar feature $h^{T}_{min}(\delta, \eta) > h^{S}_{min}(\delta, \eta)$ between the two energy surfaces as shown in Figure 10a. Thus, a singlet ground state is predicted for those isomers classified into group S, independent of the replaced heteroatoms.

On the contrary, isomer **18** causes a characteristic crossing between the two Neel state energies of $h^{T}_{min}(\delta, \eta)$ and $h^{S}_{min}(\delta, \eta)$ as shown in Figure 10b. A singlet−triplet instability would therefore be expected for isomer **18** because the crossing line gives the feature of $h^{T}_{min}(\delta, \eta) = h^{S}_{min}(\delta, \eta)$. Figure 10b also reveals that this crossing line is $2\delta^2 - 2\delta - \eta + 1 = 0$ and that the singlet−triplet instability occurs at various δ and η values along this line from the localized case ($\delta = \eta = 0.5$) to the fully delocalized ($\delta = \eta = 1$) case. Beyond this crossing line, the stable spin state is reversed from the triplet spin arrangement to the singlet spin arrangement. Thus, the possible ground-state spin multiplicity changes from the singlet state to the triplet state via the unstable state, in accordance with the values of δ and η. Nevertheless, we can say that isomer **18** prefers a triplet ground state because heteroatom substitution does not cause a large π-spin delocalization: Assuming a heteroatom B for the π spin hole and a heteroatom N for the π spin cap in isomer **18**, an ab initio UHF/6-31G** calculation gives values of at most $\eta = 0.0407$ and $\delta = 0.0169$ for the singlet state and $\eta = 0.0902$ and $\delta = 0.1739$ for the triplet state. These values are significantly smaller than those π-spin transfers (η and δ) causing the singlet−triplet instability along the crossing line of $2\delta^2 - 2\delta - \eta + 1$.

A more interesting feature is found in the π spin hole and spin cap arrangement such as isomer **20**. This isomer produces two crossings between the two energy surfaces of the singlet (LS) and triplet (HS) states; one occurs along the crossing line of $\delta = 0$, and the other occurs along that of $4\delta + \eta - 4 = 0$. The former causes the special point of $\delta_{small} = \eta_{small} = 0$ as shown in Figure 10c. This feature means that the singlet−triplet instability occurs even when the π-electron spin is significantly or completely localized ($\delta_{small} \approx \eta_{small} \approx 0$). This is also the reason that the simple Ising spin approximation can predict the singlet−triplet instability concealed in isomer **20**. We obtained the corresponding in- and out-flowings of the π-electron spin by the UHF/6-31G** calculation via B- and N-atom-replaced isomer **20**. Those values are $\delta_{small} = 0.1834$ and $\eta_{small} = 0.1158$. They seem to be slightly large, and a positive value of Δ_{TS} results numerically. Nevertheless, these values become a sufficient reason for isomer **20** to have the potential to cause the singlet−triplet instability, as the Ising spin approximation ($\delta = \eta = 0$) predicts.

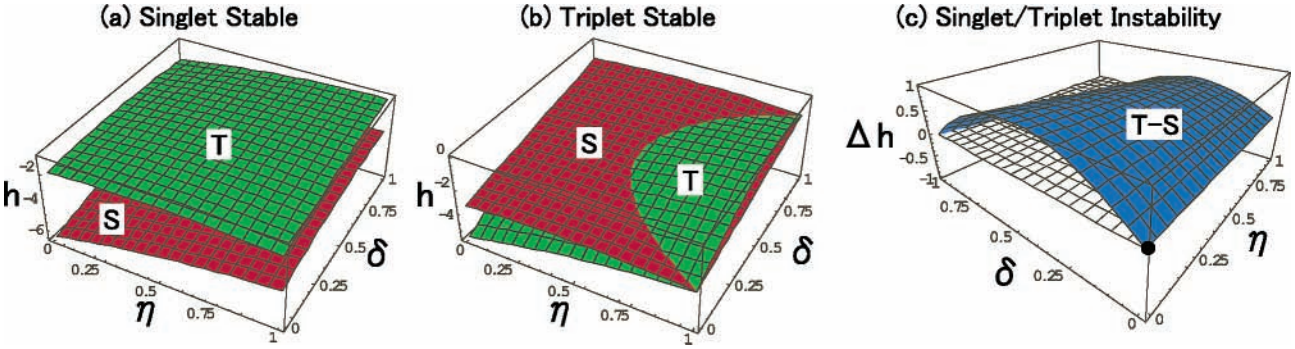

Figure 10. Calculated Neel state energies of the singlet (S) and triplet (T) states while varying the π-spin delocalizations of δ and η. We show those of isomers (a) **7**, (b) **18**, and (c) **20**, respectively. In part c, we show the difference value $\Delta h = h^{T}_{min} - h^{S}_{min}$ directly in order to represent the singlet−triplet instability more precisely.

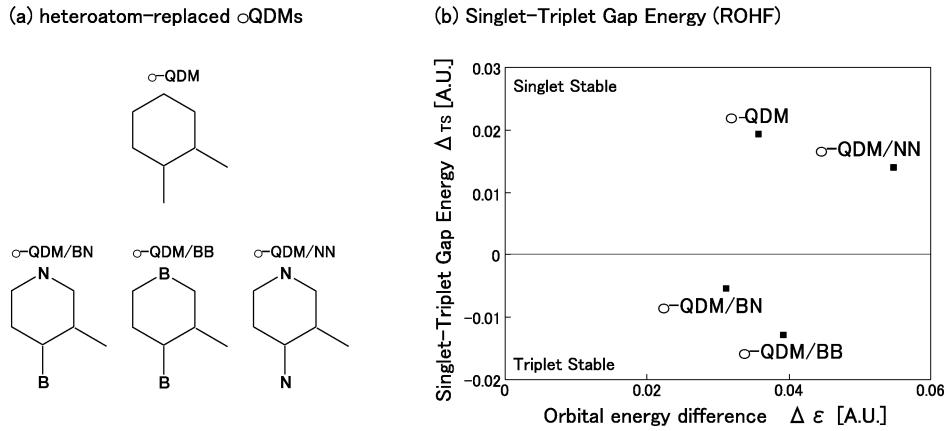

Figure 11. Illustration of (a) the heteroatom-substituted three *o*-QDMs and (b) their resulting Δ_{TS} values obtained by the ROHF/6-31G** calculations. On the horizontal axis of graph b, we show the difference in the HOMO and HOMO-1 orbital energies in the triplet state.

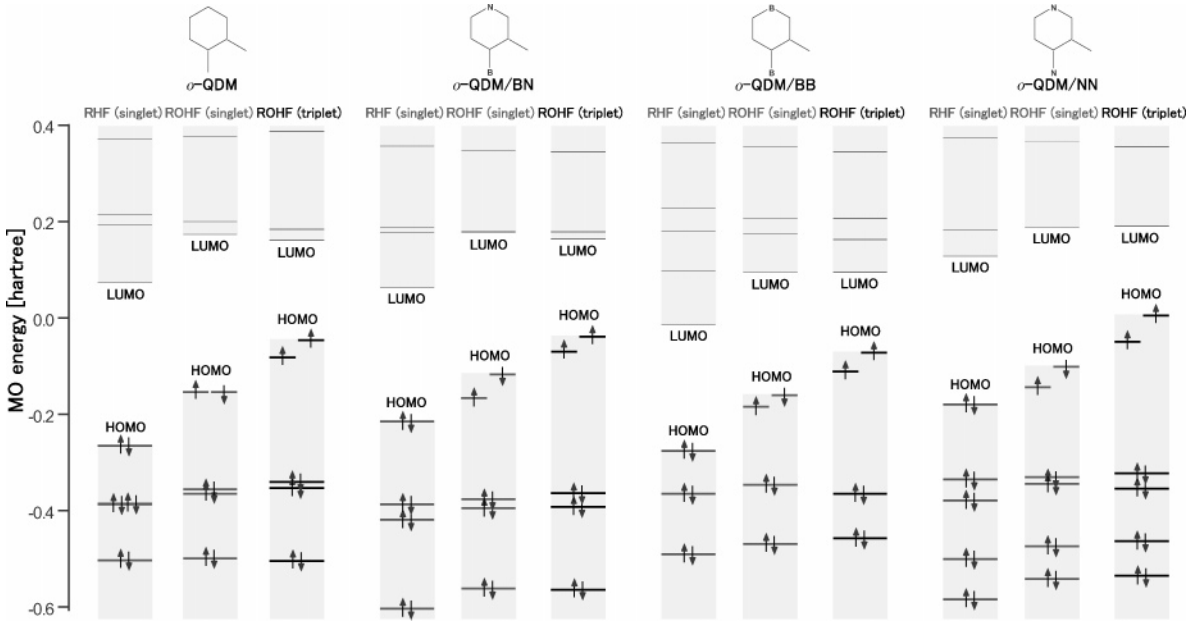

Figure 12. Illustration of the π MOs for the heteroatoms-replaced four *o*-QDMs obtained by the ROHF/6-31G** calculations.

V. Electronic Difference between π Spin-hole and Spin-cap

As mentioned in the SVB approach, ab initio HF (ROHF and UHF) calculations, and the Neel state consideration, the stable spin phase of *o*-QDM, for example, changes from a singlet state to a triplet state when the spin hole and spin cap are incorporated (isomer **1** of Figure 1). However, the SVB approach cannot distinguish the difference in the electronic nature between the spin hole and spin cap at all. The Neel state consideration also does not distinguish it explicitly, except for their spin values (δ and η). Therefore, the heteroatoms functioning as the π spin hole and spin cap are mutually commutative, and isomer **18** of Figure 1 is also expected to provide the triplet-stable phase. This stability is confirmed by ab initio HF calculations as shown in Figure 5a and b.

The electronic nature is, however, very different between the π spin hole and π spin cap. The former is produced by an excess π electron at a group IV atom (i.e., the π local pair), and the latter is produced by a π-electron deficiency at a group III atom (i.e., the complete lack of a π electron). Does such a difference then change the stable spin phases for those isomers? If so, what causes such changes? To discuss this subject, we focus on the following four ortho-type heteroatom-substituted isomers: *o*-QDM, *o*-QDM/BN, *o*-QDM/BB, and *o*-QDM/NN as shown in Figure 11a.

Figure 11b shows the resulting Δ_{TS} for these four *o*-QDMs, obtained by the ROHF/6-31G** calculations. Although all three heteroatom-substituted isomers (except for *o*-QDM) are expected to have a triplet stable state, *o*-QDM/NN is not included in this prediction, and a singlet stable phase is forecast. It is also characteristic that an increase in the number of replaced N atoms (π spin caps) enhances the stabilization of the singlet state. In Figure 12, we also show the corresponding π MOs. Although we discuss their characteristic details in Appendix A, one can notice the following features; for the above four isomers, an increase in the number of replaced N atoms causes the destabilization of the frontier states of HOMO, (HOMO-1), and LUMO, independent of its own spin multiplicity. Thus, with an increasing number of spin caps (N atoms), we can briefly conclude that the frontier states of HOMO, (HOMO-1), and LUMO shift upward.

One should, however, notice that these shifts are somewhat deceptive and that the details are individually different in accordance with the degree of the incorporated spin hole and spin cap. They are interpreted as follows: Although the *o*-QDM/

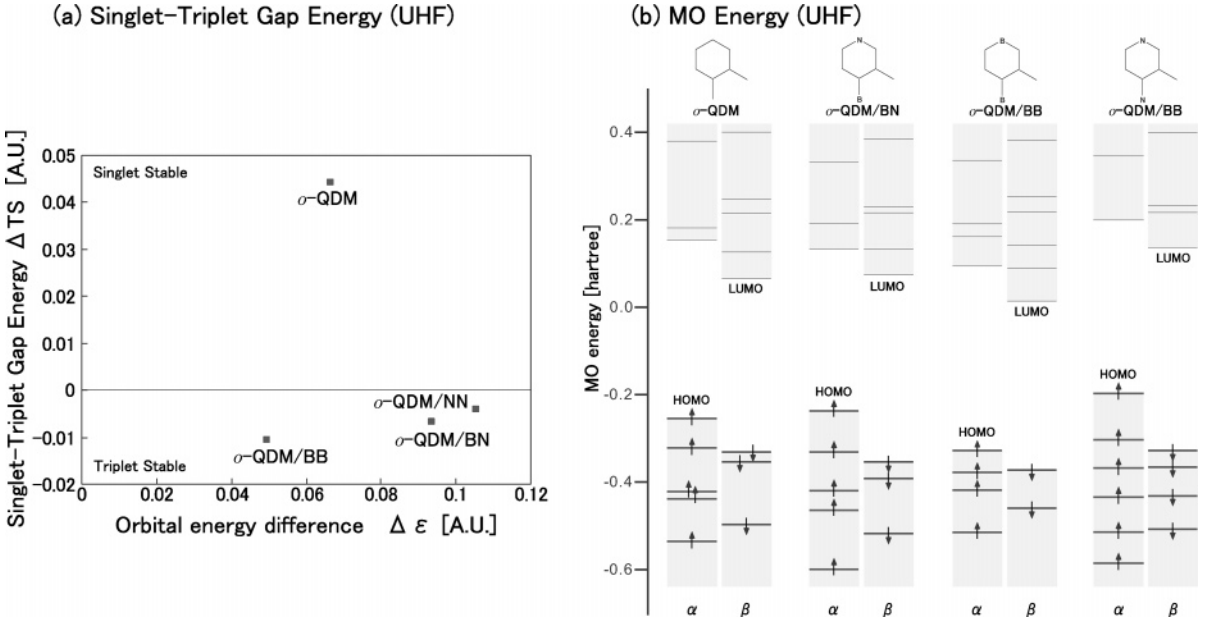

Figure 13. Resulting Δ_{TS} values for (a) the four heteroatom-replaced *o*-QDM isomers and (b) the corresponding π MOs. These values are obtained by the UHF/6-31G** calculations. On the horizontal axis of graph a, we show the difference in the HOMO and HOMO-1 orbital energies in the triplet state.

BN isomer includes both the spin hole (B) and spin cap (N), the resulting HOMO should shift upward compared with that of *o*-QDM because the 2p π on-site energy of boron (spin hole) is higher than that of carbon. However, *o*-QDM/BB includes two spin holes, by which the total π-electron number is reduced by 2 from those of *o*-QDM and the HOMO is shifted one MO lower. This change appears to be the seeming lower shift of the frontier states. On the contrary, the two excess π electrons in the *o*-QDM/NN isomer should occupy MOs one higher than for *o*-QDM/BN. This replaced occupation also causes an inevitable upward shift of the HOMO and the other frontier states. As a result, even a nonbound state is found in the HOMO state of *o*-QDM/NN. The peculiar conversion of *o*-QDM/NN to the singlet stable phase is caused by this extremely destabilized nonbound state obtained by the ROHF/6-31G** calculation (Appendix A).

The UHF/6-31G** calculations "reasonably" predict the expected result (Figure 13a); *o*-QDM/NN is now consistently classified into the triplet group, and all three replaced isomers cause a triplet stable phase. A positive slope is also found in the $\Delta\epsilon - \Delta_{TS}$ relation. In the UHF scheme, the "full" restriction for all of the (π) MO states stabilizes the individual MOs energetically, although it loses physical advantages such as being an eigenstate of S^2. The nonbound HOMO state found in *o*-QDM/NN is then stabilized so as to be a bound HOMO in this UHF result. This feature causes the stable spin phase of *o*-QDM/NN to revert from a singlet state to a triplet state (Figure 13a). One should also notice that a "sufficient" nonrestriction by the UHF scheme produces "sufficiently" stabilized occupied states, which open a Hartree−Fock (HF) gap (energy gap between the HOMO and LUMO states) widely compared with that by the ROHF scheme.

Thus, the present HF (RHF, ROHF, and UHF) calculations elucidate that the difference between the π spin hole and spin cap appears to be a shift in the frontier MO states. These calculations also reveal that such a difference is well understood by the one-electron picture (i.e., the difference in the number of π electrons and also that in the on-site energies), not by the difference in the electronic natures themselves, although the spin hole is completely different from the spin cap. This picture is, of course, quite natural because the HF calculation stands on the one-electron approximation. Nevertheless, we find the one-electron picture helpful in understanding the features of the spin hole and spin cap. The reason is as follows: in our last work,[3] we studied the possible spin state created by the spin holes in the more general polyacene system. We extended there the SVB approach to joint and disjoint π-electron chains. The combination of these results is crucial for the designing of molecular magnetism; for example, one can say that the incorporation of spin holes effectively functions to provide the HS stable state when the same number of spin caps are incorporated.

TABLE 4: Prediction of the Stable Spin State for *m*-QDM Dimers[a]

dimer	catenation	Δ_{QD}	SVB prediction
(17)−(17)	(T)−(T)	−0.03936	Q
(1)−(1)	(T)−(T)	−0.01914	D/Q
(10)−(13)	(S)−(S)	0.02666	D
(17)−(14)	(S)−(T)	0.008566	D
(8)−(20)	(S)−(S/T)	0.0002892	D/Q

VI. Consideration of the Extended System

We finally discuss how the incorporation of the spin hole and spin cap varies the possible stable spin phases in the more extended π systems. Are the SVB approach and the Neel state consideration still valid there? For the discussion of this subject, we limit the 1D catenated *m*-QDMs (poly-*meta*-quinodimethanes) by changing the catenation number $n = 2$, 3, and so on.

In the case of the heterogeneous system[22] formed by the catenation of heteroatom-replaced *m*-QDMs, the created spin hole and spin cap also cause a variety of possible spin multiplicities. We show several cases catenated by two heteroatom-replaced *m*-QDMs (Table 4). The first column identifies the kind of composed species (*m*-QDM/BN) as numbered in Figure 3. We show their own predicted spin multiplicities in the second column. The third column shows the energy difference between the doublet and quartet states obtained by the UHF/6-31G** calculations ($\Delta_{QD} = E_{quartet} - E_{doublet}$). Furthermore, we give the expected spin state predicted by the

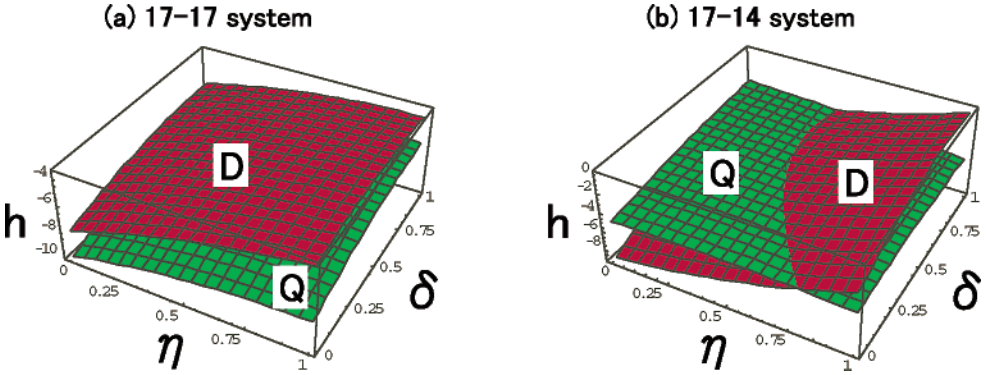

Figure 14. Calculated Neel state energies h of the doublet (D) and quartet (Q) states while varying the π-spin delocalizations of δ and η. We show those of dimers (a) **17**−**17** and (b) **17**−**14**, respectively.

SVB approach in the last column. One finds that the spin state of the resulting dimer is not always determined by the individual spin states of the composed monomers; even if the composed monomers have a unique spin state (S or T), the spin state of the polymerized dimer can cause instability between the doublet and quartet states as shown in the combination of, for example, two **1** monomers (**1**−**1**). However, it should be noticed that even in these 1D catenated forms the SVB prediction is completely coincident with the UHF result. We have also confirmed this coincidence for all of the other remaining catenated dimers.

The Neel state consideration also holds well for these catenated dimers. The computationally calculated minimum Neel state energies for the doublet (h^{D}_{min}) and quartet (h^{Q}_{min}) states are

$$h^{D}_{min}(\delta, \eta) = -8 + 6\delta + 4\eta - 2\delta^2 - 2\eta^2 - 2\delta\eta \quad (16)$$

$$h^{Q}_{min}(\delta, \eta) = -10 + 6\delta + 4\eta - 2\delta^2 - 2\eta^2 - 2\delta\eta \quad (17)$$

for dimer **17**−**17**. Similarly, for dimer **17**−**14**, the following relations are obtained:

$$h^{D}_{min}(\delta, \eta) = -9 + 3\delta + 9\eta + 3\delta^2 - 5\eta^2 - \eta\delta \quad (18)$$

$$h^{Q}_{min}(\delta, \eta) = -5 + 3\delta + \eta - \delta^2 - \eta^2 - \delta\eta \quad (19)$$

The quadraticity in the π-spin delocalization is also conserved in this extended system, and we can then show the corresponding energy surfaces in Figure 14, parts a and b, respectively. The Neel state consideration reveals that the arrangement of the spin hole and spin cap in the **17**−**17**-type dimer inherently causes the HS (quartet) stable state, where that in the **17**−**14**-type dimer changes the spin multiplicity in accordance with the values of δ and η. Alternatively speaking, in the π-spin network of the **17**−**14**-type dimer, the choice of the replaced heteroatom species changes the possible spin multiplicity, although most heteroatoms produce the LS (doublet) stable state because of their small amounts of spin in- and out-flowings.

Quite similar results are also obtained for the 1D catenated trimers in which all of the results obtained by the SVB approach, UHF/6-31G** calculations, and Neel state consideration are completely mutually coincident. However, we should emphasize that the catenation of *m*-QDM/BN monomers one-dimensionally reduces the possible cases of the HS state but increases the cases of spin instability between the LS (quintet) and HS (heptet) states. This is because the heteroatom replacement in the 1D catenation of *m*-QDM/BN oligomers lets the spin hole and/or spin cap disconnect the π-spin paths. To realize the HS ground state, one should assemble the heteroatom-replaced component so as to maintain the connection of π-spin chains or to produce roundabout π-electron paths.[23]

VII. Conclusions

In the carbon skeletal π-conjugated planar system, the replacement by the group III heteroatom causes a spin hole, and that by group V causes a spin cap. The spin hole and spin cap are expected to open a variety of possible spin multiplicities such as lower-spin (LS), higher-spin (HS), and lower-higher (L/H) unstable states, in accordance with their heteroatom arrangements.

The present HF (ROHF and UHF) calculations surely predict this possibility. The present ab initio HF calculations also forecast that the incorporation of spin holes effectively functions to provide the HS stable state, compared with the incorporation of the same number of spin caps.

To discuss the possible spin state more rationally and quantitatively, we extend the Neel state Hamiltonian by incorporating the spin delocalization. This Neel state-energy calculation classifies well the possible spin ground states and predicts the existence of three characteristic groups of LS, HS, and L/H phases.

Moreover, in the 1D catenated system, the HF results and the Neel state consideration are in agreement with the classification obtained from the SVB approach. Thus, in the 1D system having roundabout π-electron paths, the possible spin state caused by the individual heteroatom arrangement is well predicted by the SVB approach without any heavy calculations.

Acknowledgment. K.T. expresses his thanks to Professor Katsuya Eda of Waseda University for his fruitful comments and discussions and to Yuki A. Narita for his assistance.

Appendix A. π MO States by RHF, ROHF, and UHF Calculations

1. π MOs in *o*-QDM. Let us start by discussing the one-electron MO states for *o*-QDM having a singlet spin state. We show those MOs obtained by the RHF/6-31G** calculations in Figure 15a. Because *o*-QDM has a 2-fold rotational axis C_2,[16] it is divided into two equivalent butadiene parts (two C chains), and each C chain produces the four characteristic π MO states of ϕ^{C}_{i} ($i = 1-4$) as shown in Figure 15a. The resulting π MO states of *o*-QDM (Φ^{CC}_{i}) are well understood by typical orbital mixing between these composed π MOs (ϕ^{C}_{i}). Thus, one can easily understand that the HOMO ($\Phi^{CC}_{HOMO} = \Phi^{CC}_{i=4}$) corresponds to the antibonding state between the composed ϕ^{C}_{2} MOs and that the LUMO ($\Phi^{CC}_{LUMO} = \Phi^{CC}_{i=5}$) corresponds to the

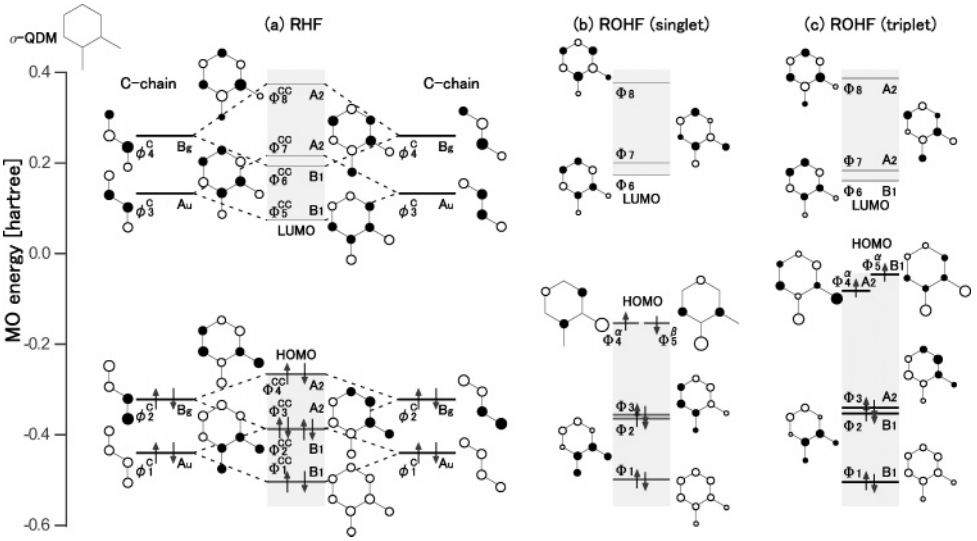

Figure 15. Illustrations of the resulting MOs (Φ_i^{CC}) of *o*-QDM having a singlet spin state (a) calculated by RHF/6-31G**, (b) those calculated by ROHF/6-31G**, and (c) those having a triplet spin state calculated by the ROHF/6-31G**. We also illustrate the resulting MOs (ϕ_i^C) of the two separate C chains calculated by RHF/6-31G**.

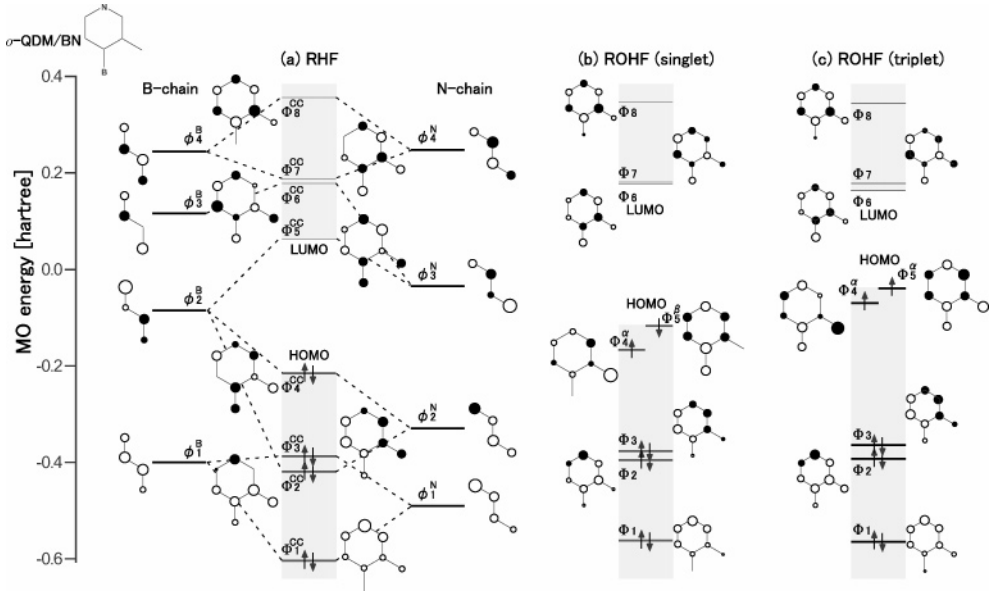

Figure 16. Illustration of the resulting MOs (Φ_i^{BN}) of *o*-QDM/BN having a singlet spin state (a) calculated by RHF/6-31G**, (b) those calculated by ROHF/6-31G**, and (c) those having a triplet spin state calculated by the UHF/6-31G**. We also illustrate the resulting MOs of the two separate chains (ϕ_i^B, B chain; ϕ_i^N, N chain) calculated by RHF/6-31G**.

bonding state between the composed ϕ_3^C MOs because of 8 π ($= 4n$, $n = 2$) electrons in *o*-QDM.

When the restriction of the α and β orbitals in the HOMO state is removed (ROHF singlet state), the HOMO state is changed from that obtained by the RHF calculation (hereafter represented as the RHF−HOMO), as shown in Figure 15b. One should notice that the orbital coefficients (Φ_4^α and Φ_4^β) appear to be opposite for the α and β spins but at intervals of the atoms. Therefore, two electrons having opposite spin never overlap mutually because the nonrestriction lets two electrons redistribute to minimize their inter-electron repulsive energy. One should further notice that the peculiar form of *o*-QDM causes NBMO-like orbital character in these states. Thus, the unrestricted Φ_4^α and Φ_4^β states are also accidentally degenerate. The lack of bonding character also shifts the resulting HOMO upward.[24]

Figure 15c shows the resulting MO states of *o*-QDM having a triplet spin arrangement, obtained by the ROHF/6-31G** calculation. It is found that the Φ_5^α state conserves its orbital character of the RHF-LUMO state and that Φ_4^α conserves that of the RHF-HOMO state; that is, we can draw a well-known simple image for the ROHF triplet state in which two electrons having the same spin individually occupy the HOMO and LUMO states obtained by the RHF scheme with less electron redistribution. This is because two electrons occupying these two states need not redistribute explicitly to optimize their inter-electron repulsion in the triplet state because of their mutual orthogonality. This feature is also caused by the fact that the one-electron stabilization caused by forming the RHF-MOs is significant in *o*-QDM and that it overcomes the inter-electron repulsive destabilization even in this triplet state. The exchange interaction between the above two electrons in the Φ_5^α and Φ_4^α states enhances this simple occupation.

2. π MOs in Heteroatom-Replaced o-QDMs. The heteroatom B and/or N replacement causes the following two changes in the above π MO states. One is the change in orbital mixing

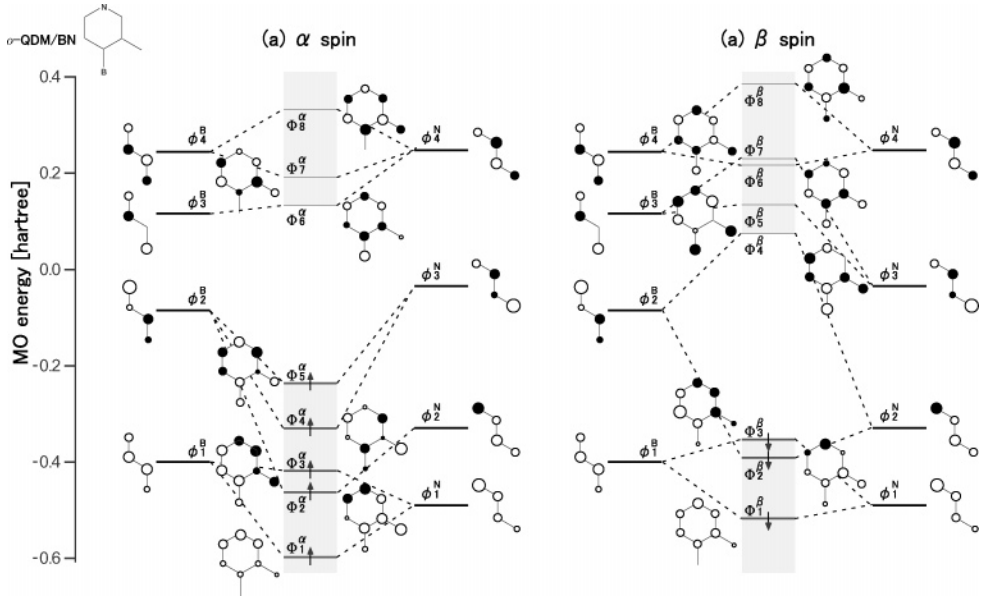

Figure 17. Illustration of the resulting MOs (Φ_i^{BN}) of *o*-QDM/BN having a triplet spin state calculated by UHF/6-31G**. We separately show the UHF-MOs having an α spin (a) and those having a β spin (b).

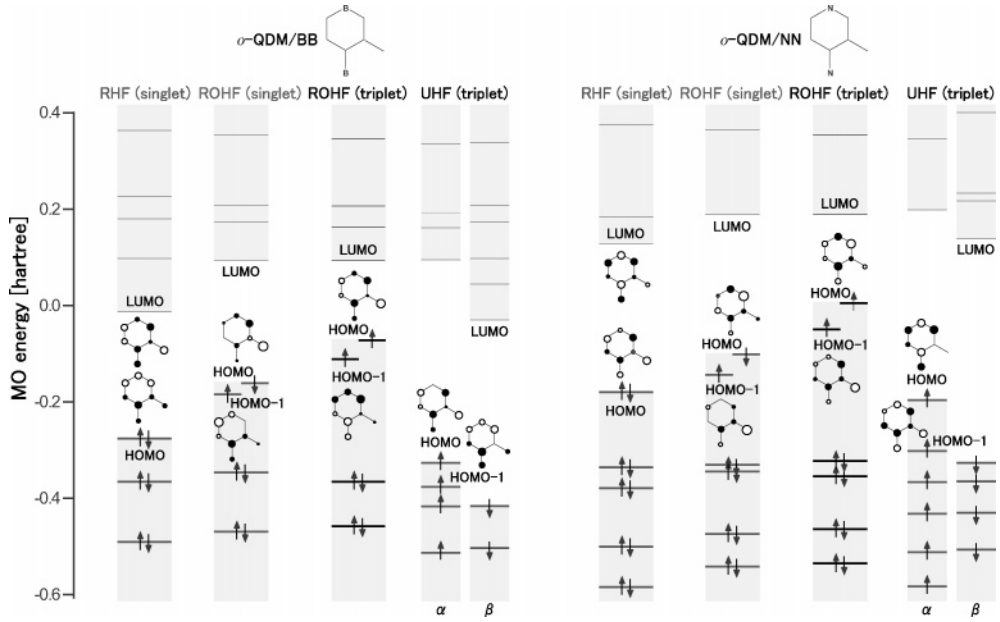

Figure 18. Illustration of the resulting MOs Φ_i^{BB} and Φ_i^{NN} obtained by RHF/6-31G**, ROHF/6-31G**, and UHF/6-31G** calculations. We also illustrate the resulting MOs of the two separate chains (ϕ_i^B, B chain; ϕ_i^N, N chain) calculated by RHF/6-31G**.

due to the change in the on-site energies of the replaced heteroatom species; the composed π MO ϕ_i^μ (μ = B, C, and N chains and $i = 1-4$) changes its own π MO state ϵ_i^μ, in accordance with the atomic on-site energies of B-, C-, and N-replaced atoms ($\epsilon_N < \epsilon_C < \epsilon_B$). The other is that the individual π MO coefficient freely changes not only its value but also its sign because of the C_s point group symmetry. Nevertheless, one should notice that the obtained MOs can be basically understood by the bonding or antibonding between the decomposed two chains of the N chain and/or the B chain.

a. o-QDM/BN. We show the resulting RHF π MOs for singlet *o*-QDM/BN in Figure 16a. The typical bonding and antibonding hybridization between constituent MOs ϕ_i^B and ϕ_i^N is found in the resulting Φ_1^{BN}, Φ_2^{BN}, and Φ_3^{BN}. The symmetry lowering due to the heteroatom replacement causes only a numerical difference in the resulting orbital coefficients. On the contrary, the HOMO and LUMO are different from those for *o*-QDM, respectively. The heteroatom replacement changes the eigenstates of the composed (B and N) chains. The N atom produces the lower 2*p* on-site energy, and the B atom produces the higher one. Therefore, the constituent π MO of ϕ_3^N is energetically close to that of ϕ_2^B, and a slightly complicated hybridization occurs. The HOMO state includes the bonding nature between ϕ_2^B and ϕ_3^N states in addition to the antibonding nature between ϕ_2^B and ϕ_2^N states, and the LUMO state consists of antibonding between the ϕ_2^B and ϕ_3^N states. Thus, although the π-electron number is conserved to be 8 in *o*-QDM/BN, one can find some difference in the orbital nature of the frontier states, HOMO (Φ_4^{BN}) or LUMO (Φ_5^{BN}), from those in *o*-QDM.

When the restriction of the α and β orbitals in the HOMO state is removed (ROHF singlet state), a redistribution of electrons is also found, but the resulting patterns are different from those found in *o*-QDM; an electron localizes at the different

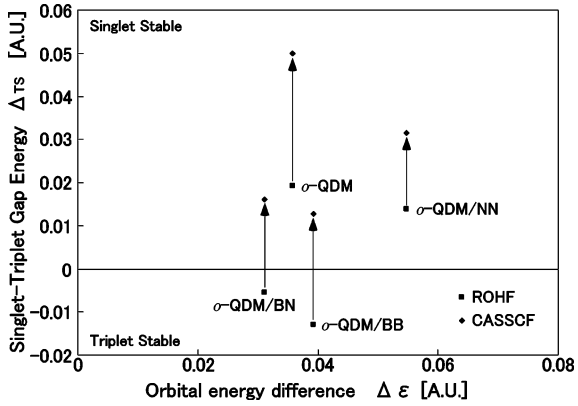

Figure 19. Resulting Δ_{TS} values for the four heteroatom-replaced *o*-QDM isomers. These values are obtained by the CASSCF/6-31G** calculations. On the horizontal axis, we show the difference in the HOMO and HOMO-1 orbital energies obtained from ROHF/6-31G** calculations.

exocyclic atom in accordance with the difference in the spin (Figure 16b). Moreover, the symmetry lowering due to B and N heteroatom replacement diminishes the NBMO-like character in these HOMO states and removes the accidental degeneracy. However, similar to the *o*-QDM case, the ROHF calculation also estimates the higher total energy (by 0.004 au) as well as the destabilized HOMO state compared with those obtained from the RHF calculation. In Figure 16c, we also show the MO states for the triplet spin arrangement obtained by the ROHF calculation. One can find the common correspondence in which the resulting Φ_5^{α} and Φ_4^{α} respectively correspond to the LUMO and HOMO obtained by the RHF calculation.

The π MO states obtained by the UHF/6-31G** calculation (Figure 17) are further complicated but basically understood by the similar orbital mixing between the two composed chains. The doubly occupied UHF-MOs ($\Phi_{i=1-3}^{\alpha(\beta)}$) completely coincide with those RHF- and ROHF-MO states. The energetic approach between the constituent MOs of ϕ_3^{N} and ϕ_2^{B} similarly causes additional orbital mixing. Thus, for the α spin orbitals, additional bonding is added to $\Phi_{i=4}^{\alpha}$, and antibonding character is induced in $\Phi_{i=5}^{\alpha}$ (Figure 17a). Furthermore, one can find that a larger HF gap opens between the HOMO and LUMO states in the UHF calculation because the "complete" nonrestriction for the opposite spins stabilizes the individual MO remarkably compared with those obtained by the ROHF calculation. It is also characteristic that the UHF result shows a larger energy difference between the HOMO and HOMO-1 compared with that obtained from the ROHF result.

b. o-QDM/BB and o-QDM/NN. Two B-atom replacements in *o*-QDM/BB reduce the total number of π electrons from those of *o*-QDM by 2. Therefore, the RHF-HOMO of the singlet *o*-QDM/BB (Φ_{HOMO}^{BB}) is expected to correspond to the third RHF-MO of *o*-QDM (Φ_3^{CC}, Figure 15a) or of *o*-QDM/BN (Φ_3^{BN}, Figure 16a). However, the resulting Φ_{HOMO}^{BB} corresponds rather to Φ_2^{CC} (or Φ_2^{BN}) as shown in Figure 18a. This is because the nested relation between two MOs of Φ_2 and Φ_3 found in *o*-QDM (and *o*-QDM/BN) is resolved in *o*-QDM/BB because of the change in the atomic on-site energies from the N to the B atom. On the contrary, the RHF-LUMO state corresponds well to the Φ_4^{CC} state, except for a slight discrepancy in the resulting coefficients.

The nonrestriction of the α and β spin orbitals in the HOMO state of the singlet *o*-QDM/BB (ROHF) causes the redistribution by which the resulting Φ_3^{α} and Φ_4^{α} orbitals are similar to those

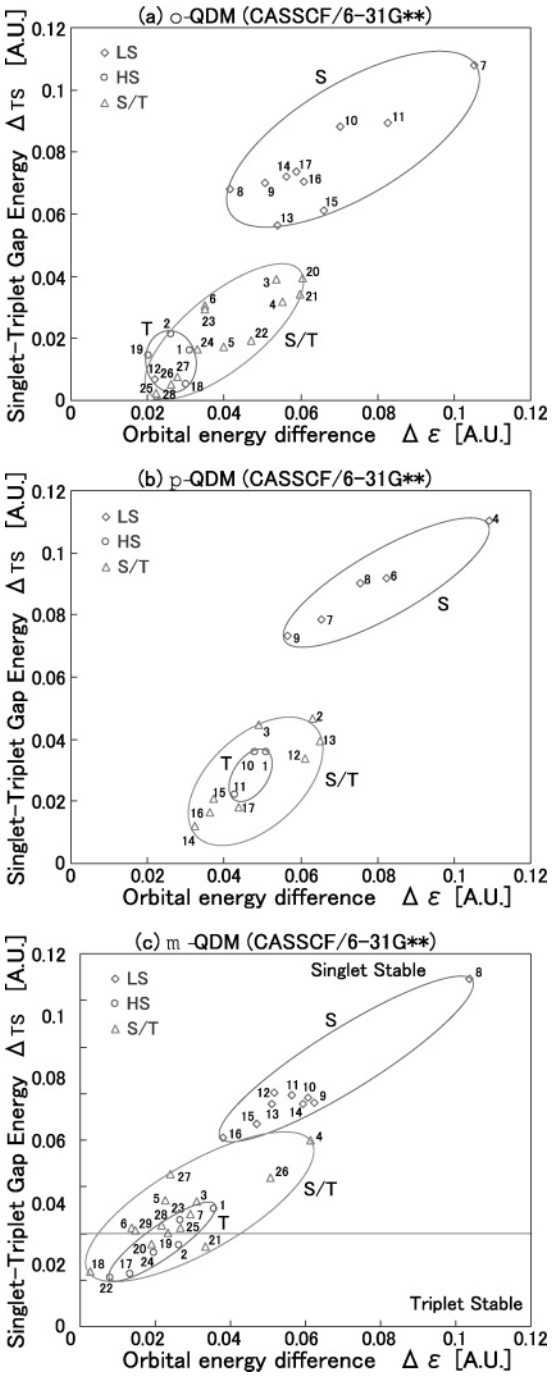

Figure 20. Resulting Δ_{TS} values for the heteroatom-replaced isomers of the (a) ortho type, (b) para type, and (c) meta type. These values are obtained from CASSCF/6-31G** calculations.

of the RHF-HOMO and -LUMO, respectively. This feature is in contrast to those in *o*-QDM or *o*-QDM/BN, in which the HOMO and HOMO-1 of the ROHF result are completely different from the LUMO and HOMO of the RHF result. In the triplet state, on the contrary, common correspondence is conserved between the ROHF-HOMO and RHF-LUMO and between the ROHF-HOMO-1 and RHF-HOMO. A considerably uniform redistribution in these two states induces a larger exchange term.

The two N-atom replacements in *o*-QDM/NN increase the total number of π electrons by 2. Therefore, the RHF-HOMO Φ_{HOMO}^{NN} of the singlet *o*-QDM/NN is expected to correspond to the RHF-LUMO (Φ_5^{CC}) of the singlet *o*-QDM (or Φ_5^{BN}). This feature is confirmed by the bonding character between the two

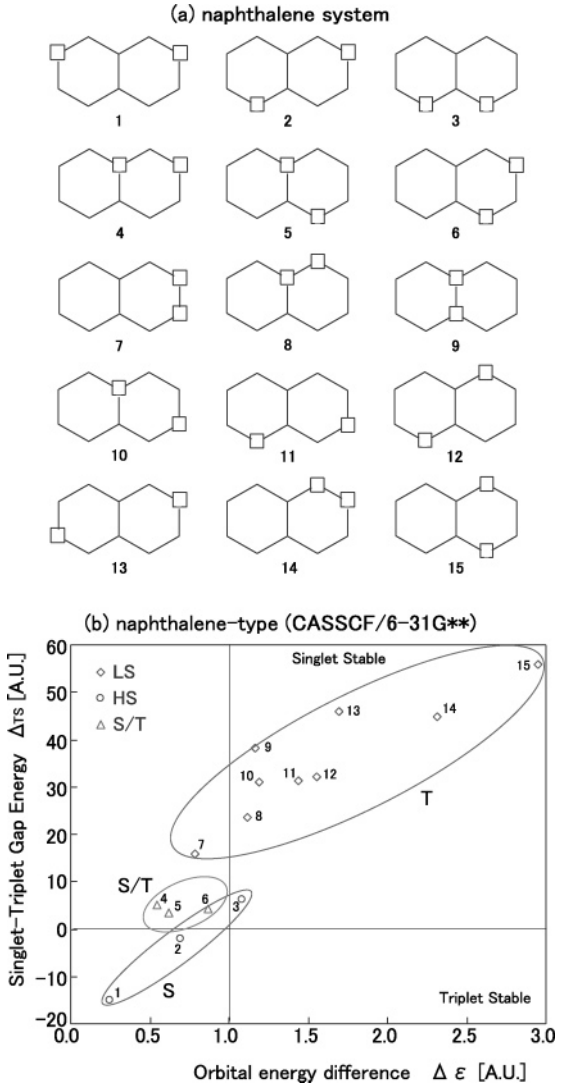

Figure 21. Resulting Δ_{TS} values for the naphthalene-type π-conjugated system in which two π spin holes are bored by the two B-atom replacements. Values are obtained from CASSCF/6-31G** calculations.

ϕ_3^N MOs, although their values and the sign of the MO coefficients are slightly varied. We also find that the RHF-LUMO state basically corresponds to the antibonding state between these two ϕ_3^N MOs. The nonrestriction for the α and β spin orbitals in the HOMO state (ROHF) of the singlet *o*-QDM/NN causes an exceptional redistribution (Figure 18b). The correspondence between the ROHF-HOMO and RHF-LUMO is small, but that between the ROHF-(HOMO-1) and RHF-HOMO is not found anymore. In Figure 18, we also show the resulting UHF π MOs both for *o*-QDM/BB (a) and *o*-QDM/NN. The characteristic correspondence of the UHF-HOMO and -HOMO-1 states with the RHF-LUMO and -HOMO is also recognized.

Appendix B. π-Electron Correlation Induced by the π Spin Hole and Spin Cap

How does the π-electron correlation induced by the π spin hole and spin cap change the above stable spin phase? To discuss this subject briefly, we incorporated these π-electron correlations via the configuration interaction (CI) of eight π electrons under eight π orbitals by the complete active space self-consistent field (CASSCF) method with a 6-31G** basis set (CASSCF/6-31G**). We show the Δ_{TS} CASSCF results for these four ortho-type isomers (Figure 19). A significant similarity is found between those results obtained by the CASSCF and ROHF calculations (Figure 11b); with an increasing number of π spin caps (replaced N atoms), these isomers prefer to be a singlet stable phase. A peculiar change to the singlet stable phase is also found for *o*-QDM/NN. This similarity is quite natural because the CASSCF calculation is based on the linear combination of the ROHF Slater determinants while changing their electron configurations. Thus, in the CASSCF scheme, the π-electron correlation is reduced as a positive but uniform shift in Δ_{TS} values. Paradoxically, this uniformity indicates an indistinguishability between the π spin hole and spin cap: An analogous π-electron correlation occurs within the present CASSCF scheme, independent of the difference in the present π spin-hole (B) and π spin-cap (N) species. Moreover, the resulting positive shift of $\Delta_{TS} \approx 0.02$ au by the present CASSCF calculation leads all *o*-QDM isomers to favor a singlet stable phase.

On the basis of these CASSCF features, we can discuss our calculated energy differences Δ_{TS} for (a) *o*-, (b) *p*-, and (c) *m*-QDM isomers as shown in Figure 20. The π-electron correlation by the present CASSCF/6-31G** calculations removes the triplet spin stable phase from ortho and para isomers. The three characteristic spin phases appear in meta isomers only. However, one should carefully reach this conclusion. As mentioned in Figure 19, the CASSCF calculation causes a Δ_{TS} shift including some drawbacks. They are generated by the unreliable stabilization of the occupied MO states based on the ROHF scheme because all of the MOs except for the HOMO are still restricted. Thus, some treatments beyond the CASSCF approach (e.g., the full-CI approach, etc.) should be carried out for a more accurate discussion.

References and Notes

(1) Iwamura, H.; Izuoka, A. *J. Chem. Soc. Jpn.* **1987**, *4*, 595. Iwamura, H. In *New Synthetic Methodology and Functionally Interesting Compounds*; Yoshida, Z., Ed. Kodansha: Tokyo, 1986.

(2) Ito, K. Ed. *Molecular Magnetism* (*Gakkai Syuppan*) 1996, and references there in.

(3) Takahashi, N.; Takeda, K. *J. Phys. Soc. Jpn.* **2002**, *71*, 2295. Takahasi, N. Ph.D. Thesis, Waseda University, Tokyo, Japan, 2003.

(4) Borden, W. T.; Davidson, E. R. *J. Am. Chem. Soc.* **1977**, *99*, 4587.

(5) Ovchinnikov, A. A. *Theor. Chim. Acta* **1978**, *47*, 297.

(6) Döhnert, D.; Koutecký, J. *J. Am. Chem. Soc.* **1980**, *102*, 1789.

(7) Flynn, C. R.; Michl, J. *J. Am. Chem. Soc.* **1974**, *96*, 3280.

(8) Kato, S.; Morokuma, K.; Feller, D.; Davidson, E. R.; Borden, W. T. *J. Am. Chem. Soc.* **1983**, *105*, 1791.

(9) Fort, R. C.; Getty, S. J.; Hrovat, D. A.; Lahti, P. M.; Borden, W. T. *J. Am. Chem. Soc.* **1992**, *113*, 7549.

(10) Karafiloglou, P. *Int. J. Quatum Chem.* **1984**, *25*, 293.

(11) Longuet-Higgins, H. C. *J. Chem. Phys.* **1950**, *18*, 265.

(12) The presence of the heteroatoms removes the zero-MO coefficients causing the NB state. Thus, one cannot distinguish between the disjoint and nondisjoint MOs because the strict NB states disappear.

(13) By extending the meaning of Kekulé structures, we applied the LH rule to the present heteroatomic system. We have drawn the extended Kekulé structures with two double bonds to each N atom whenever the atom has two or more C atoms as neighbors because the two local pairs of π electrons on the N and the two electrons on the neighboring C atoms all pair to form a four-electron singlet. An earlier extension of the LH rule to the case of homoatomic species has been carried out by Borden and Davidson: Borden, W. T.; Davidson, E. R. *Acc. Chem. Res.* **1981**, *14*, 69.

(14) For example, consider the following recent review: Klein, D. J. *Valence Bond Theory*; Cooper, D. L., Ed.; Theoretical and Computational Chemistry; Elsevier: Amsterdam, 2002; Vol. 10, p 447.

(15) Ivanciuc, O.; Klein, D. J.; Bytautas, L. *Carbon* **2002**, *40*, 2063. Ivanciuc, O.; Bytautas, L.; Klein, D. J. *J. Chem. Phys.* **2002**, *116*, 4735.

(16) The molecular structure of the present heteroatom-replaced QDM isomers has been optimized assuming C_{2v} or C_s point group symmetries in accordance with the corresponding form; most of them have a point group symmetry of C_s, but **12** and **14** of *p*-QDMs and also **5** and **27** of *m*-QDMs

can have a point group symmetry of C_{2v} in addition to C_s. For these latter isomers, we have carried out both forms and have taken the more stable form.

(17) We have calculated the total energies for the singlet spin arrangement both by the RHF and ROHF calculations, and we then determined the HF singlet state by obtaining the energetically more stable one.

(18) Hartmann, H. *Z. Naturforsch., A* **1947**, *2*, 259. Malrieu, J.-P.; Maynau, D. *J. Am. Chem. Soc.* **1982**, *104*, 3021. Maynau, D.; Malrieu, J.-P. *J. Am. Chem. Soc.* **1982**, *104*, 3029.

(19) Klein, D. J. J.; Alexander, S. A.; Matsen, F. A. *J. Chem. Phys.* **1982**, *77*, 3101.

(20) The Heisenberg-model spin Hamiltonian $\hat{H}$ is given as follows: $\hat{H} = -\Sigma_{i,j}\, 2J_{ij}\hat{\boldsymbol{S}}_i \cdot \hat{\boldsymbol{S}}_j$ where J_{ij} is the exchange integral and $\hat{\boldsymbol{S}}_i$ is the total spin operator on the ith site. We here assume that the system has a completely 2D planar form; therefore, π electrons are well defined. Consequently, it is reasonable that all of the spins originate from these individual π electrons and that the Ising spin approximation is valid. Thus, the spin components S_x and S_y causing the nondiagonal elements are ignored in the Hamiltonian, and eq 3 is obtained.

(21) An exchange integral between two adjacent π electrons should be negative so as to arrange their π-electron spins antiparallel in the valence bond scheme.

(22) In the case of a homogeneous system composed of *m*-QDMs, the following features are well known theoretically and experimentally. When two *m*-QDMs are catenated one-dimensionally, both the LH and SVB methods predict the quartet (Q) ground state. The UHF/6-31G** calculation also supports the quartet state being more stable than the doublet state by 0.0715 hartree. Similarly, when three *m*-QDMs are catenated, all of the one-electron considerations of the LH, SVB, and HF (UHF/6-31G**) predict the quintet-spin ground state. Thus, the following inductive formula is obtained for the spin multiplicity of the *n* catenated *m*-QDMs: $S = (n + 1)/2$.

(23) We consider the case of the naphthalene-type π-conjugated system in which two π spin holes are formed by the two boron atom replacements. This is because the HS state tends to appear by the spin holes rather than the spin caps, as mentioned in the text. The existence of the HS states in this π system is also supported by the CASSCF/6-31G** calculation (Figure 21). Moreover, for an extended π system such as a polyacene, we can classify the possible spin-stable states and generalize their prediction by considering the topological connection and disconnection of the π-spin chains. Those results will be reported in the next paper.

(24) The orbital restriction generally causes an energetic destabilization due to the interelectron repulsion. However, the stabilization of the one-electron MO states induced by the bonding and/or antibonding nature is so significant in *o*-QDM as to overcome this interelectron destabilization. Consequently, one can also find that this type of stabilization in the one-electron MO leads to a stabilization in the total energy; the result by the present RHF/6-31G** calculation is 0.002 hartree lower than that by the ROHF/6-31G** calculation.

(25) [a]We also show those spin states predicted by the SVB approach, ab initio UHF/6-31G** calculations, and the Neel state consideration.

(26) [a]$\Delta_{QD} = E_{quartet} - E_{doublet}$ is the energy difference between the quartet and doublet spin arrangement obtained by the UHF/6-31G** calculation in hartrees.